Materials Chemistry and Physics 293 (2023) 126967

Contents lists available at ScienceDirect

Materials Chemistry and Physics

journal homepage: www.elsevier.com/locate/matchemphys

Assessment of flexible pristine CdS film electrodes in photoelectrochemical light-to-electricity conversions

Majd Sbeah [a], Ahed Zyoud [a], Maen Ishteiwi [a], Muna Hajjyahya [a], Naoual Al Armouzi [b], Naser Qamhieh [c], Abdul Razack Hajamohideen [c], Samer Zyoud [d], Hamza H.S. Helal [a], Heba Bsharat [a], Heba Nassar [a], Mohammed H.S. Helal [e], Hikmat S. Hilal [a,*]

[a] SSERL, College of Sciences, An-Najah National University, Nablus, P400, Palestine
[b] Industrial Engineering Laboratory, Faculty of Sciences and Technologies, Sultan Moulay Slimane University, Beni-Mellal, 23000, Morocco
[c] Department of Physics, United Arab Emirates University, Al-Ain, United Arab Emirates
[d] College of Humanities and Science, Department of Mathematics and Basic Science, Ajman University, United Arab Emirates
[e] Department of Electrical and Computer Engineering, Birzeit University, Birzeit, Ramallah, Palestine

HIGHLIGHTS

- Flexible pristine CdS films are deposited onto ITO/PET substrates by CBD and ECD methods.
- Films are optimized by deposition time & layer, annealing temperature and cooling rate.
- Flexible CBD-CdS/ITO/PET electrode competes with rigid CdS systems in PEC performance.
- High PEC efficiency and stability are achieved by film 125 °C annealing and quick cooling.

GRAPHICAL ABSTRACT

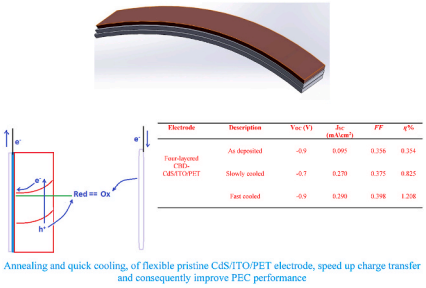

Annealing and quick cooling, of flexible pristine CdS/ITO/PET electrode, speed up charge transfer and consequently improve PEC performance

ARTICLE INFO

Keywords:
Flexible pristine CBD-CdS films
Flexible ITO/PET substrates
PEC
Efficiency & stability

ABSTRACT

Compared to rigid CdS/glass electrodes, flexible pristine CdS electrodes have not been described in photo-electrochemical (PEC) based light-to-electricity conversions, despite wide descriptions of their preparations and characterizations. CdS film electrodes, deposited on flexible tin-doped indium oxide/polyethyleneterephthalate (ITO/PET) substrates, have been prepared here by both chemical bath deposition (CBD) and electrochemical deposition (ECD). The film PEC characteristics have been investigated here. With a very low thickness, the flexible ECD-CdS electrode fails to show measurable PEC performance. On the other hand, with higher film thickness, the CBD flexible electrode shows soundly high PEC performance. To further improve PEC characteristics of the flexible CBD-CdS/ITO/PET electrodes, various parameters have been varied, such as number of deposition cycles, annealing temperature, cooling rate and type of redox couple. Among the studied films, the four-layered CBD-CdS/ITO/PET film, annealed at 125 °C and quickly cooled, exhibits highest PEC performance and stability, with conversion efficiency higher than 1.2% in polysulfide redox couple. The results show that the flexible CBD-CdS/ITO/PET electrode may compete with earlier rigid CdS film electrodes deposited on fluorine doped tin oxide/glass substrate.

* Corresponding author.
E-mail addresses: hshilal@najah.edu, hikmathilal@yahoo.com (H.S. Hilal).

https://doi.org/10.1016/j.matchemphys.2022.126967
Received 16 August 2022; Received in revised form 9 October 2022; Accepted 29 October 2022
Available online 31 October 2022

1. Introduction

Homo- and hetero-junction p-n type photovoltaic (PV) devices are currently used at wide commercial scale due to their high conversion efficiency and stability. However, p-n based PVs are prepared at the millimeter scale thickness using relatively large amounts of starting materials. They also demand special preparation conditions. Easy-to-deposit semiconductor polycrystalline film electrodes, with nanometer scale thickness, are emerging to save cost and environment and to minimize starting material amounts [1]. Metal chalcogenides MX (M = Cd, Cu, Zn, etc.; X = O, S, Se and Te) are one major class of materials widely studied in polycrystalline film electrodes. Typically, the MX films are prepared by various methods including physical vapor deposition (PVD), chemical vapor deposition (CVD), sputtering, laser deposition, together with other simple methods such as electrochemical deposition (ECD), chemical bath deposition (CBD), onto fluorine-doped tine oxide (FTO) and tin-doped indium oxide (FTO) pre-deposited onto glass substrates. A widely studied example of such systems is CdS with a wide range of band gap values from 2.0 to 3.0 eV depending on preparation method, conditions and film characteristics [2–5]. The band gap is suitable for visible solar radiations, which makes CdS useful in solar energy applications. CdS films were deposited onto rigid FTO/glass substrates and investigated in PEC applications, with the possibility to enhance their conversion efficiencies once treated properly [6–8].

To expand their future applications, CdS film electrodes were prepared onto tin-doped indium oxide (ITO) pre-deposited on flexible substrates. Polyethylene terephthalate (PET), polydimethyl siloxane (PDMS), Kapton HN, Upilex-S and others were described [9,10]. Despite their advantages, flexible solar cells still exhibit low performance compared to other rigid counterparts, and demand extensive study. Research is active on flexible cupper-indium-gallium-sulfide (CIGS) based systems to improve their PEC performance [11]. Flexible CdS/CdSe film electrodes were reported in PEC studies [12]. On the other hand, other pristine flexible film electrodes, such as those of CdS, were not described in PEC studies. Flexible nano-rod CdS@CNTs, coated on stainless iron-mesh electrodes, were described in hydrogen production [13]. Laser ablation was used to prepare Al/CdS/Al solid film electrodes to use as photodetectors, and the system showed sound photo-response in photodetectors [14]. Flexible solid state PdS/CdS-based heterojunction solar cells with efficiency higher than 4% were described earlier [15]. Other researchers prepared and characterized CdS films on flexible substrates using various depositions but without describing the PEC characteristics [16,17]. Preparation of other pristine CdS films, onto flexible substrates by the simple CBD, were also described [2,16,18–21]. The ECD method was not described for flexible CdS electrodes. To our knowledge, pristine CdS film electrodes deposited onto flexible substrates, have not been reported in light-to-electricity conversion using known PEC processes, in which the semiconductor electrode is brought in direct contact with a solution redox couple. The present work describes CBD- and ECD-prepared pristine flexible CdS film electrodes in PEC for the first time.

PET has been chosen here, as a substrate for CdS films, due to its low cost, availability and high transmittance to visible solar light, despite its low tolerance to processing temperatures above 125 °C [9]. On the other hand, CdS film characteristics may be improved by annealing at moderate temperature, as reported earlier [22,23]. In fact, low- and medium-band gap semiconductor materials may undergo permanent deformations by heating at high annealing temperatures [22–24]. Therefore, to avoid any negative effects on the CdS or the PET, the CdS/PET films should be annealed at mild temperatures, which further adds to process advantages.

In earlier studies we described the CBD and ECD prepared CdS films on FTO/glass substrates with relatively low efficiencies [6–8]. While the ECD films were not enhanced by annealing, the CBD film characteristics were slightly enhanced [7]. The as-deposited ECD film already exhibited high crystallinity and morphology that were lost upon heating, without being reclaimed on cooling. On the other hand, the CBD film characteristics, with relatively low uniformity and crystallinity, were slightly enhanced by annealing. The earlier results indicated that in case of CdS films, and other low-to medium-band gap metal chalcogenide film electrodes, annealing at moderate temperatures should be considered [23]. Moreover, cooling rate effect [23] should also be carefully considered, in similar materials.

In the present study, pristine CdS films have been deposited onto flexible ITO/PET substrates, aiming at producing flexible CdS film electrodes for PEC applications. No similar studies were reported to our knowledge. The goal is to see if such flexible films can exhibit PEC efficiency that competes with rigid FTO/glass-based counterparts. Moreover, the films involve the environmentally hazardous Cd ions [25] and should be stabilized to photo-corrosion under PEC conditions. Therefore, stabilizing the flexible CdS film is another goal of this work.

Two different methods of preparation are described, the ECD and CBD. As assumed earlier, the ECD method yields films with high crystallinity, uniformity and adherence to the substrate. On the other hand, the CBD method yields films with more suitable thickness to absorb light but with less crystallinity and surface uniformity. Therefore, both methods are described here. The prepared flexible CdS films will be annealed at mild temperatures, in order to avoid affecting the PET sheets or the semiconductor films themselves. Effects of annealing and cooling rate on film PEC performance and stability will be studied. The study will comparatively answer the following questions: Is it possible to prepare flexible CdS/ITO/PET films by simple CBD and ECD methods? Which preparation method yields electrodes with highest PEC performance? How do the flexible CdS films compare with earlier reported CdS/FTO/Glass rigid electrodes? Will annealing the flexible CdS films further improve their properties and consequently their PEC characteristics? Can the film stability under PEC conditions be improved by carefully controlled annealing and cooling rate? To our knowledge, these issues were not described in earlier studies.

2. Experimental

2.1. General materials and equipment

Organic solvents have been purchased in high purity from Riedel-DeHaen. Starting materials (thieourea, Cadmium (II) Acetate Dihydrate ($C_4H_{12}CdO_6$), $CdCl_2{\cdot}2H_2O$, NH_3, $LiClO_4$, Na_2S, NaOH, elemental sulfur, NH_4Cl, HCl, acetic acid and $Na_2S_2O_3$ have been purchased from Merck, Frutarom or Aldrich. Indium tin oxide coated polyethylene terephthalate (ITO/PET) sheets have been purchased from Merck (with surface resistivity 60 Ω/sq, $1x10^{-3}$-inch-thick, and more than 78% transparency in the visible).

For electrochemical depositions a Potentiostat C.S. model Electrochemical Workstation has been used. PEC experiments have been conducted using a computer-controlled CorrTest Electrochemical Workstation CS350 Potentiostat/Galvanostat. Solid state electronic absorption spectra have been measured for the CdS films on a Shimadzu UV-1601 spectrophotometer, with ITO/PET used for baseline correction. A JEOL JSM-6700F FESEM microscope has been used to measure the scanning electronic micrographs. Electronic dispersive spectroscopy (EDS) has been measured on the same FESEM equipment, which is located at the UAE University, Al-Ain. For X-ray diffraction (XRD) measurements, an Analytical X'Pert PRO X-ray diffractometer (XRD), with CuKα (λ = 1.5418 Å), at the UAE University, Al-Ain, has been used. A 50 W halogen solar simulator lamp has been used as a source of radiation.

2.2. CdS film preparations

Two various methods have been used to prepare CdS/ITO/PET films, as described below. In each case the ITO/PET substrates (1 × 4 cm^2) have been cleaned as described by known methods. The substrates have

been rinsed with deionized water (DW), sonicated for 10 min in a detergent solution, rinsed with DW several times and carefully dried under nitrogen streams.

2.2.1. CBD-CdS/ITO/PET

The procedure is based on earlier method described for CBD-CdS onto FTO/Glass [26]. A 20.5 mL bath, with pH 10.0, containing DW (2.5 mL), $CdCl_2$ solution (2.50 ml, 0.358 M), NH_4Cl solution (10.0 ml, 0.60 M) and NH_3 solution (3.0 ml, 25%), has been prepared and heated at 75–80 °C. Then a thiourea solution (2.5 ml, 0.089 M) has been added. The ITO/PET substrates have been partially dipped (1×3 cm^2 exposed) inside the bath for 30 min. The resulting films have then been rinsed with DW, dried and stored for further characterization and use.

For multi-deposition, the same procedure has been repeated on the prepared CdS/ITO/PET films for 2, 3, 4, 5 and 6 times. The various as-deposited films have been examined in PEC, and the fourth time deposited film exhibits the highest conversion efficiency, as described in Section 3 below. Therefore, it has been chosen over others for further treatment as described below in Section 2.3.

2.2.2. ECD-CdS/ITO/PET

ECD deposition procedure has been performed as described earlier for CdS films deposited onto FTO/Glass [27,28]. A stirred solution of cadmium (II) acetate dihydrate ($C_4H_{12}CdO_6$), (10 ml of 0.598 M), $Na_2S_2O_3$ (10 ml of 0.148 M), $LiClO_4$ (~0.741 g) and DW (30 ml) has been prepared. To the solution has been added HCl(aq) dropwise to control the pH value at ~2.5. The solution temperature has then been raised to 90 °C and maintained. The pre-cleaned ITO/PET substrate has then been partially inserted inside the stirred solution as a working electrode. A platinum sheet has been used as a counter electrode, whereas an SCE electrode has been used as a reference. Care has been taken to avoid contact between copper wires and the solution. Electrodeposition has been conducted using a DC current at −0.9 V (vs. NHE) and continued for 2 h, but the resulting CdS film is too thin to detect or characterize. It exhibits very low PEC performance to measure, and has therefore been excluded from the study.

2.3. Film characterization

Solid state electronic absorption spectra, XRD patterns, SEM micrographs and SEM data have been measured on equipment listed in Section 2.1 above. To measure the approximate film specific surface area (SSA), the method of acetic acid adsorption described earlier [29] has been followed. Optical band gap values have been approximately measured using the Tauc plot method [30] described in Equation 1

$$(\alpha h\upsilon) = \beta\left(h\upsilon - E_g\right)^n \tag{1}$$

where α refers to absorption coefficient; n is 2 assuming a direct band gap for CdS [5]; h is the Planck's constant; ν is the radiation frequency; β is an optical constant and E_g is the band gap value.

The film thickness has been measured by three methods. In the gravimetric method, the difference in mass between the CdS/ITO/PET and the substrate ITO/PET has been measured, but the results are not reliable and have not been considered. In the spectrophotometric methods, the measured absorbance values have been used to find film thickness. Equation (2), which relates film thickness e to absorbance and absorptivity, is substituted in Equation (1), to yield Equation (3) that has been used to measure film thickness [31] in one method.

$$\alpha = \left(\frac{2.3}{e}\right)A \tag{2}$$

where A refers to absorbance;

$$(Ahv)^2 = \left(\beta\frac{e}{2.3}\right)^n.(h\upsilon - E_g) \tag{3}$$

Moreover, the film thickness has been measured using the envelope method from the measured solid state electronic absorption spectra as described earlier [32,33]. The two spectroscopic methods show film thickness values with ±10% variations. The results are consistent in terms of thickness variation tendencies among various films. Therefore, average thickness values have been considered for each film.

2.4. Annealing

Based on PEC results described below, the four-layered CdS/ITO/PET film has been modified by annealing here. The goal is to see if film properties and PEC characteristics can be further enhanced by annealing.

As described in Section 1 above, based on earlier literature, only low annealing temperatures (100, 125 and 150 °C) have been chosen here. Annealing has been conducted under nitrogen atmosphere in a thermostated tube furnace pre-heated at the desired temperature. The film has been placed inside a Pyrex glass tube with inlet and outlet for the slow inert gas stream, and the tube has then been placed inside the furnace for 15 min.

The film has been cooled to room temperature by either of two methods, fast cooling and slow cooling. In slow cooling, the furnace has been switched off and left to reach room temperature in the course of more than 120 min. In fast cooling, the glass tube has been withdrawn from the furnace (at the given temperature) and quenched with water bath in less than 5 min.

2.5. PEC experiment

PEC experiments have been performed inside a thermostated (room temperature) two-electrode cell with the CorrTest Electrochemical Workstation. The CdS/ITO/PET electrode has been used as the working electrode, and a platinum sheet as a counter electrode. The potentiostat internal cell has been used as reference electrode by connecting it with the platinum counter electrode. The internal cell has been calibrated vs. NHE reference electrode. The potential values are thus measured relative to NHE.

The PEC cell, has been charged with the redox couple solution that has been stirred with a stream of N_2 (99.999%) for 5 min. Two redox couple-electrolyte aqueous systems have been attempted, namely S (0.10 M)/Na_2S (0.10 M)/NaOH (0.10 M) or [$K_3Fe(CN_6)$] (0.10 M)/[$K_4Fe(CN_6)$] (0.10 M)/$LiClO_4$/(0.10 M). The former redox couple exhibits higher PEC performance, and therefore it has been used in measuring the PEC results unless otherwise stated.

The PEC experiment has then been started after the stirring was stopped and the nitrogen gas stream lifted and kept above the electrolyte solution to prevent contamination with air. The applied potential has been scanned in the range −1.5 – 0.0 V (vs NHE) at a scan rate 50 mV/s. The photocurrent-potential (*J-V*) plots have been measured under constant illumination intensity (0.0086 W/cm^2) at the working electrode surface. The low radiation intensity is intentionally chosen to avoid any overheating at the electrode. PEC characteristics, such as open circuit potential (V_{OC}) in V vs NHE, short circuit photo current density (J_{SC}) in A/cm^2, fill factor (*FF*) and conversion efficiency (η%) have all been extracted from the *J-V* plots. The conversion efficiency has been calculated from the photo J-V plots, using Equation (4):

$$\eta\% = \frac{FF\ V_{OC}\ J_{SC}}{P_{in}} \tag{4}$$

where P_{in} is incident intensity in W/cm^2.

Electrode stability under PEC conditions has been studied by keeping the working electrode under continuous exposure to radiation (0.0086 W/cm^2) at applied potential 0.0 V (vs. NHE) in the S (0.10 M)/Na_2S (0.10 M)/NaOH (0.10 M) redox couple. Values of J_{SC} have been measured and plotted vs. time.

3. Results and discussion

3.1. General

Two types of flexible film electrodes have been prepared here, namely ECD-CdS/ITO/PET and CBD-CdS/ITO/PET films. The ECD-film is too thin and could not be characterized or studied in the PEC experiments, and has therefore been ruled out from characterization study. Compared to earlier ECD prepared CdS/FTO/Glass films [6], which were characterized by various methods, the present ECD-CdS/ITO/PET film is too thin to observe here. The difference between the two ECD film thicknesses is presumably due to the resistivity value difference between the substrates FTO/Glass and the ITO/PET, being ~7 and 60 Ω/sq respectively. The high substrate resistance may prevent formation of CdS films with enough thickness to characterize. This could explain the lack of literature reports on ECD prepared CdS/ITO/PET films, compared to other methods such as laser ablation [14] or CBD described above. In future studies of ECD-flexible CdS film electrodes, it is strongly recommended to re-consider the issue of film thickness. Methods to improve film thickness, by careful choice of the organic substrate, electrolyte type and others, need to be developed.

The CBD-CdS electrodes have been characterized prior to PEC study. In micro-spherical CdS materials the reported specific surface area (SSA) was ~27 m^2/g [34]. In the present study the CBD-CdS/ITO/PET films exhibit SSA values of 50–80 m^2/g, depending on number of layers and on annealing treatment, *vide infra*.

3.2. Electronic absorption spectra

3.2.1. - As deposited CBD-CdS/ITO/PET films

Mono-layered CBD-CdS films have been prepared using various deposition times namely 30, 60, 90, 120, 150 and 180 min. The as-deposited films have been studied by electronic absorption spectroscopy using the ITO/PET substrate for base line correction. Fig. 1 (1) summarizes the electronic absorption spectra measured for the as-deposited films before any treatment. Each film shows an absorption maximum at about 491 nm. The Figure shows that the film deposited in 120 min exhibits higher absorbance than the other films deposited in shorter times. However, after 120 min, the absorbance also decreases, indicating that the 120 min is the optimal deposition time. Literature [35,36] showed that CBD CdS/Glass film thickness increased with deposition time up to a certain limit, after which the film thickness decreased. These discussions are revisited in this Section, *vide infra*.

From Fig. 1(2), the Tauc plots show that the optical energy band gap values, for various films deposited in 30, 60 and 90 min are, are ~2.1 eV. For film deposited in 120 shows a smaller band gap of ~1.8 eV. The values are in agreement with earlier reported values for other CdS films [2,3]. The films deposited in longer times, 150 and 180 min, exhibit band gap values that are too small and unrealistic. The smaller band gap values indicate variations in film properties deposited in longer times as reported earlier [37], as discussed below.

Based on these results, the strategy here has been focused on preparing CBD-CdS/ITO/PET films deposited in different layers, as described in Section 2, allowing 30 min deposition time for each layer. Electronic absorption spectra have been measured for the CBD-CdS/ITO/PET films with various layers. The results are summarized in Fig. 2 (1).

Fig. 2(1) shows that four-layered film (total deposition time 120 min) exhibits higher absorbance than other counterparts, which is consistent with monolayered film deposited in 120 min. The Tauc plots for various films are shown in Fig. 2(2). One-, two- and three-layered films exhibit Tauc relations, with low slopes, yielding rough band gap values of ~2.0 eV or higher. On the other hand, five- and six-layered films have too small band gaps to be realistic. The four-layered film exhibits a clear and a conclusive Tauc relation with a band gap value of 2.0 eV, which resembles literature values for CdS/ITO/Glass films [5,38,39]. Based on these results, the four-layered CdS/ITO/PET films have been considered for further study.

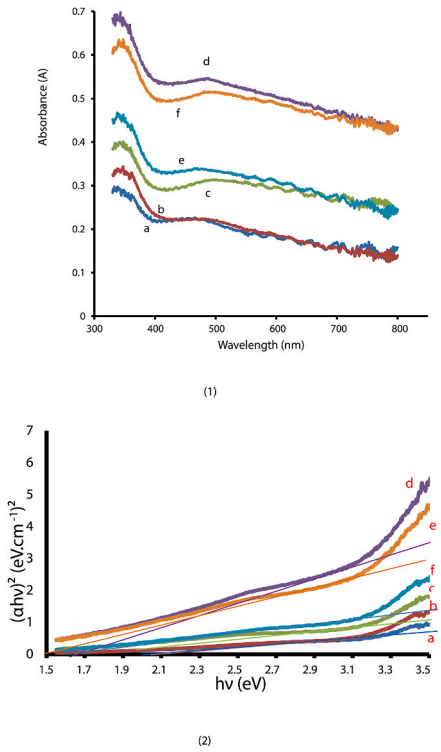

Fig. 1. Optical properties measured for mono-layered CBD-CDS/ITO/PET films. (1) Electronic absorption spectra and (2) Tauc plots. Preparation times a) 30 min, b) 60 min, c) 90 min, d) 120 min e) 150 min and f) 180 min.

Effects of multi-layers or deposition time of CBD-CdS/ITO/PET on film thickness has not been earlier reported, while similar studies were made on CBD-CdS/Glass films [36]. The four-layered film exhibited higher thickness (~61.5 nm) than in one-, two- and three-layered films, with ~11, 20 and 25 nm, respectively. This is understandable, as more layers should yield thicker films. However, after 4 layers, namely five and six layers, the films exhibit lower thickness values of ~45 nm.

The results are consistent with earlier literature. Ouachtari et al. showed that CBD-CdS/FTO/Glass mono-layered film thickness and crystallinity were improved with longer deposition time up to 60 min, after which the film thickness and crystallinity were lowered [35]. The authors explained thickness lowering by saturation of the produced film after some time, where more of the solid material dissolved in the CBD solution. In addition to deposition time, CdS/Glass films thickness, morphology and optical properties were all controlled by the number of deposition layers. In multi-layered CBD CdS/Glass films, Ouafi et al. showed that the film thickness increased with layer number, and with deposition time, to certain extents and then decreased. The results were again explained based on saturation and dissolution of the solid films after certain deposition layers and times [36]. With its favorable properties, the four-layered CBD-CdS/ITO/PET film has been singled as the material of choice here.

3.2.2. - Annealed CBD-CdS/ITO/PET

As described above, CdS/ITO/PET should be annealed with care to avoid negative effects on the PET film characteristics. Control experiments have been made on naked flexible ITO/PET substrates, to test their stability to annealing. The naked substrates show stability to temperatures up to 125 °C with no noticeable change in their mechanical and spectral properties.

Moreover, the medium band gap CdS film should be treated at moderate temperatures only [23]. Therefore, only a moderate

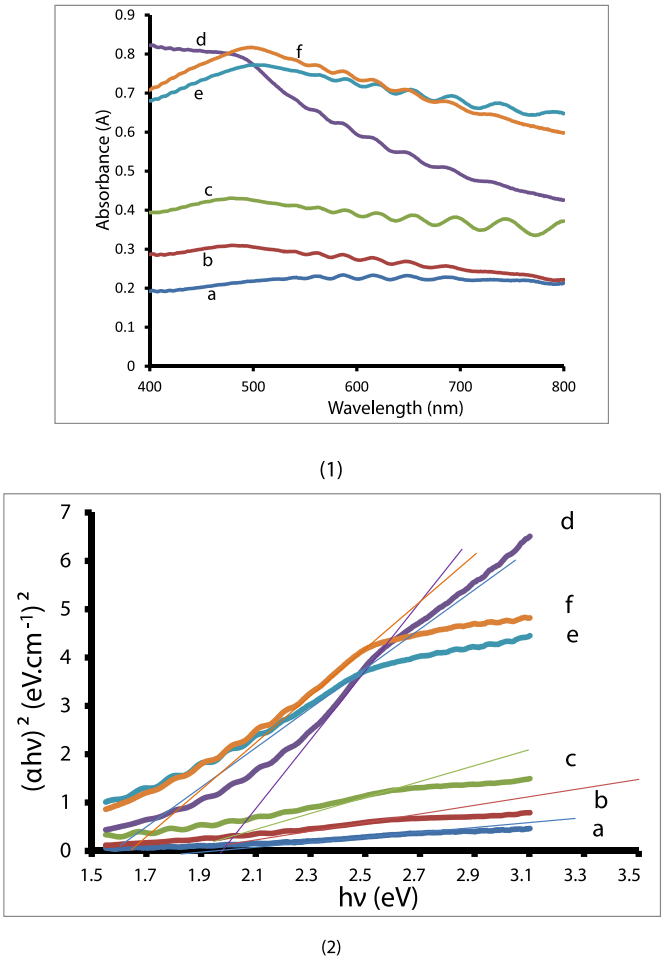

Fig. 2. Spectral properties measured for CBD-CDS/ITO/PET films deposited in various layers. (1) Electronic absorption spectra and (2) Tauc plots. Layer numbers a) one, b) two, c) three, d) four, e) five and f) six layers.

temperature 125 °C has been used here for the four-layered CBD-CdS/ITO/PET films. Fig. 3(1) and (2) summarize the effect of annealing and cooling rate on both spectra and Tauc plots for CBD-CdS/ITO/PET films. Annealing at 125 °C shows little effect on the four-layered film spectrum especially when quickly cooled.

Both the as-deposited and the quickly cooled films exhibit Tauc plots showing measurable band gap values. The as-deposited film has a band gap value of 2.0 eV, while the quickly cooled film shows a smaller band gap of 1.9 eV. The slowly cooled film shows a band gap value that is difficult to measure and too small to be acceptable. In slow cooling, the annealed film exhibits higher change in its spectral characteristics. In slow cooling, exposure to heat occurs for time long enough to affect the film characteristics. Similar behaviors were reported for metal chalcogenide films deposited on FTO/Glass substrates, where slow cooling rate could be advantageous [26] or disadvantageous [40] depending on the system under study and the annealing temperature [23]. With flexible substrates here, it is disadvantageous to slowly cool the flexible film.

The annealed four-layered CBD-CdS/ITO/PET film at 125 °C involves densification. The thickness, measured as described in Section 2, is lowered from ~62 nm to ~46 nm for quickly cooled film, and to ~40 nm for slowly cooled film. Film densification is expected by annealing as described earlier [31]. Higher densification is expected in the slowly cooled film due to longer exposure to heat, as described above. This is further corroborated by the measured SSA values being ~80, ~62 and 56 m^2/g, for the as deposited, quickly cooled and slowly cooled films, respectively.

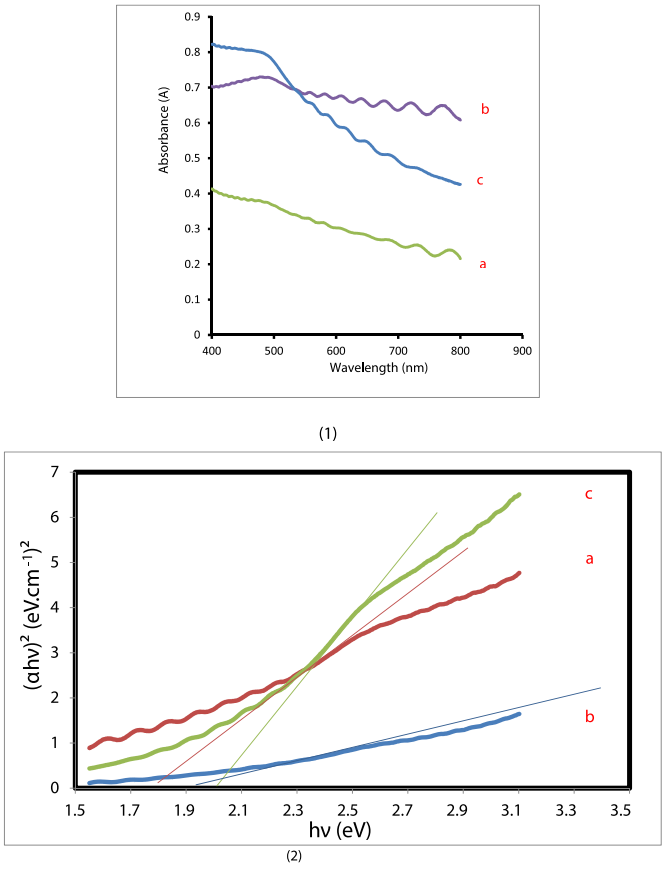

Fig. 3. Effect of annealing on measured optical properties for four-layered CBD-CdS/ITO/PET films. (1) Electronic Absorption Spectra and (2) Tauc plots. a) Annealed at 125 °C and slowly cooled, b) Annealed at 125 °C and quickly cooled and c) As-deposited.

3.3. XRD patterns

3.3.1. - As-deposited film

The four-layered CBD-CdS/ITO/PET film has been further characterized by XRD, as summarized in Fig. 4(a). The Figure shows the CdS layer reflections only, and the characteristic (222) and (400) reflections at $2\theta = 30.52$ and 35.37°, respectively, known for ITO are not observed [41,42].

The CdS film XRD patterns have been compared with earlier literature [39,43,44]. The as-deposited CBD-CdS/ITO/PET film exhibits a number of reflections as described in Table 1. The XRD pattern indicates the presence of CdS mixed cubic and hexagonal phases, with the latter being the predominant one. The face centered cubic phase reflections (111), (220) and (311) can be observed at $2\theta = 26.0$, 44.0 and 52.6°, respectively. Other reflections at $2\theta = \sim 12.7$, 23.4 and 46.5° refer to the minor hexagonal phase. Earlier literature indicated that with no high temperature treatment, CdS films mainly exhibited the cubic structure [45]. The patterns show that the as-deposited CBD-CdS film involves nano crystallites. Based on the Scherrer equation [45], the average crystallite diameter (D) for the cubic crystallites in the film is ~4.9 nm, with preferential orientation (111). Table (1) summarizes structural properties for the film, based on literature [46,47].

3.3.2. - Annealed film

Effect of annealing and cooling rate on four-layered CBD-CdS/ITO/PET film crystal structure has been studied, Fig. 4 (b) and (c). The film has been annealed at 125 °C, for the reasons discussed above, and cooled either slowly or quickly. Similar to the as-deposited film, XRD patterns show that both annealed films exhibit crystallites of mixed cubic and

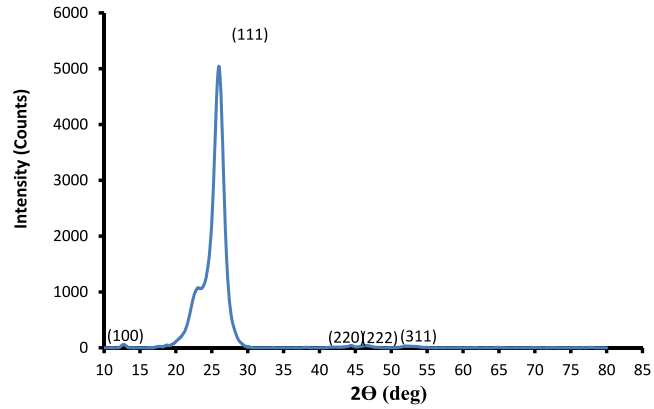

(a)

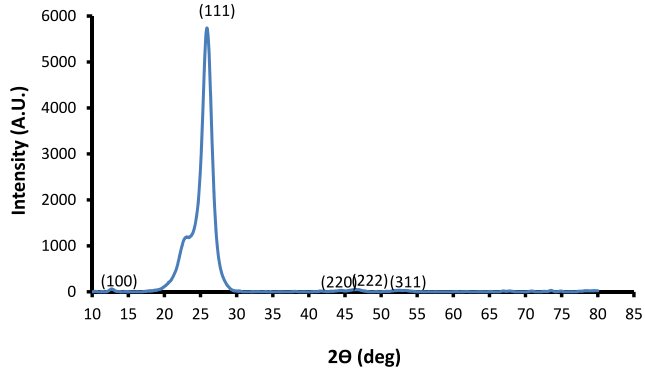

(b)

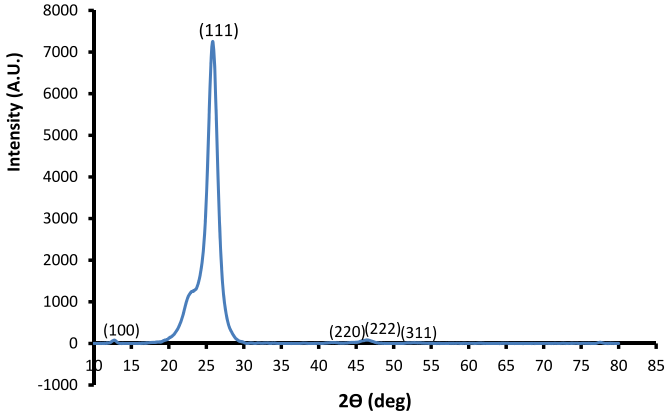

(c)

Fig. 4. XRD patterns measured for various four-layered CdS/ITO/PET films. (a) as-deposited film, (b) annealed at 125 °C and slowly cooled, and (c) annealed at 125 °C and quickly cooled.

Table (1)
Summary of particle size values for four-layered CBD-CdS/ITO/PET films in the predominant cubic phase.

2θ°	Plane (hkl)	Crystallite diameter (nm)		
		As-deposited	Annealed quickly cooled	Annealed slowly cooled
26.0	111	6.0	6.0	5.9
44	(220)	4.5	4.5	4.5
52.6	311	4.2	4.1	4.2
Average		4.9	4.9	4.9

hexagonal CdS phases, with the former being the dominant phase. The approximate average crystallite diameter (D) for slowly and quickly cooled films, being ~ 4.49 nm for each, is similar to the as-deposited film, Table 1. In either case, the annealing has no effect on the CdS crystallite size itself, Table 1 as the low temperature is not enough to cause intimate sintering between smaller crystallites.

As the annealing temperature is not high enough, no phase change is observed by annealing, as the cubic phase remains dominant. Literature [30,45] showed that low temperature treatment of CdS films yields the cubic phase, while at higher temperatures (300 °C or higher) the hexagonal phase dominates. Therefore, at moderate temperature here, the cubic phase should dominate.

A closer look at Fig. 4 shows that annealing affects film crystallinity and disorder. Reflection height ratio for the (111)/(100) in each film, shows that the ratio value is higher for the quickly cooled film than for the as-deposited film, indicating higher crystallinity in the former. The slowly cooled film also shows higher ratio than the as-deposited film, which again indicates improved crystallinity by annealing. However, the ratio in the quickly cooled film is higher than in the slowly cooled film, which indicates that the quickly cooled film exhibits highest crystallinity among the series. The results indicate that annealing enhances the CdS film crystallinity within the crystallites, but the quick cooling is preferable. With prolonged heating, in case of slow cooling, the crystallinity is lowered. Similar results were reported in other semiconductor film electrodes [23].

3.4. SEM micrographs

SEM surface images have been measured for four-layered CBD-CdS/ITO/PET films, Fig. 5. The as-deposited film, Fig. 5(a), shows a surface with flat shaped agglomerates of ~50 nm in diameter. Each agglomerate involves smaller crystallites of ~4.9 nm as depicted from XRD patterns. The EDS results show many elements, due to contamination of the equipment, with ~Cd/S atomic ratio 7/9. The higher atomic ratio for S should make the film p-type conductor, but the PEC results below indicate otherwise. Similar behavior was reported earlier for CdS films with higher S atomic ratio but still have n-type conduction [48]. The reason is that the excess sulfur is not in its elemental form, but in other impurity compound form, in the film.

Fig. 5(b) shows that the annealed and quickly cooled four-layered CdS/ITO/PET film, involves flat-shaped agglomerates of ~60 nm in diameter. Each agglomerate involves smaller crystallites of ~4.9 nm, as confirmed by XRD patterns. Compared to the as-deposited film, annealing caused growth in the agglomerate sizes, but not in crystallite size, as confirmed by XRD patterns above. The moderate annealing temperature is not enough to cause complete sintering between the crystallites themselves into larger ones, but only causes agglomerate growth here. Within the agglomerate, the crystallites retain their original sizes. The EDS results measured for the annealed film shows Cd/S atom ratio of 5/6, which is slightly higher than in the as-deposited film.

Compared to quickly cooled counterpart, the annealed and slowly cooled four-layered CdS/ITO/PET film, Fig. 5(c), exhibits larger agglomerates ~200 nm in diameter. This is due to longer time of exposure to temperature in case of slow cooling, which causes more agglomerate growth than in fast cooling. Again, the average crystallite diameter ~4.9 nm, measured by XRD patterns, does not change in case of slow cooling. This because the annealing temperature is not enough to cause crystallite sintering. The EDS also shows Cd/S atom ratio of about 5/6 that is slightly higher than the as-deposited film.

3.5. PEC studies

As described in Section 1, PEC characteristics were not earlier reported for pristine CdS films prepared onto ITO/PET flexible substrates, which makes the present results as a pilot study. As stated above, the PEC study is restricted to the CBD-CdS/ITO/PET films. The very thin

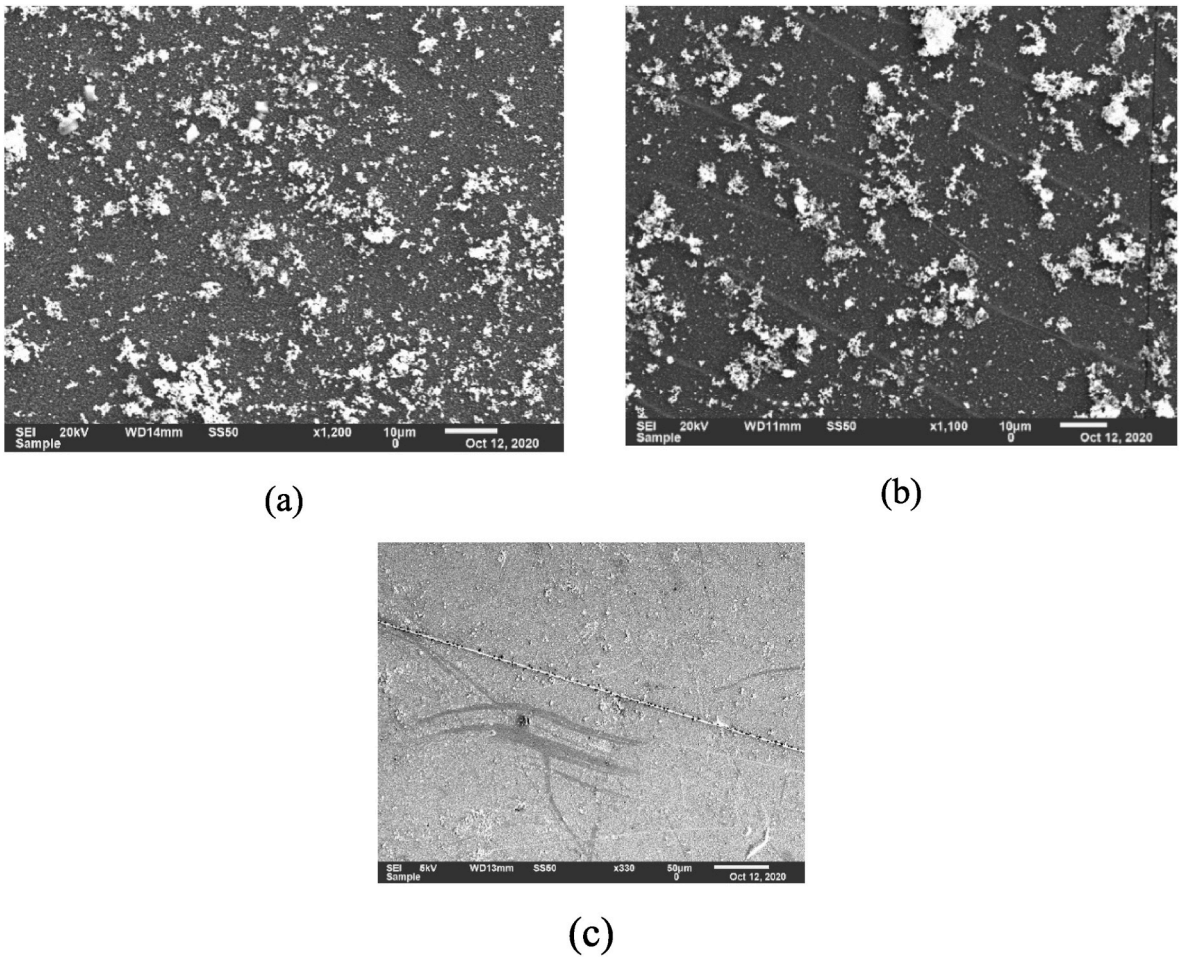

Fig. 5. SEM micrographs measured for four-layered CBD-CdS/ITO/PET films. (a) as deposited, (b) annealed at 125 °C and quickly cooled, and (c) annealed at 125 °C and slowly cooled.

ECD-CdS/ITO/PET films have been excluded, although their ECD-CdS/FTO/Glass counterparts were earlier investigated [7], Section 3.1.

All as-deposited and annealed CBD-CdS/ITO/PET films have been tested for PEC study. Two redox couples have been examined namely S/Na_2S/NaOH and $[K_3Fe(CN_6)]/[K_4Fe(CN_6)]/LiClO_4$, where the former shows higher PEC performance and has thus been used unless otherwise stated. The studied PEC characteristics involve photo *J-V* plots, FF, J_{SC}, V_{OC} and η%.

3.5.1. As-deposited electrode

Photo *J-V* plots have been measured for as deposited mono-layered CBD-CdS/ITO/PET electrodes prepared during various deposition times (30, 60, 90, 120, 150 and 180 min). Among the various films, the one prepared in 120 min shows highest PEC performance, with J_{SC}, V_{OC}, FF and η% values 0.035 mA/cm^2, -0.71 V, 0.625 and 0.174%, respectively. The conversion efficiency is lower than earlier reported value 1.16% for mono-layered CBD-CdS/FTO/Glass electrode [6]. This is expected from flexible solar cells compared to rigid counterparts [11]. However, enhancing the PEC performance has been attempted here by using multi-layered CBD-CdS/ITO/PET films with various layers 1, 2, 3, 4, 5 and 6. Effect of layer number on CBD-CdS/ITO/PET film PEC characteristics has been studied. The four-layered film exhibits highest PEC characteristics among the series, with J_{SC}, V_{OC}, *FF* and *η%* values being 0.095 mA/cm^2, -0.9 V, 0.33, 0.35%, respectively, as shown in Table 2. The *η%* value is higher than that reported in earlier mono-layered CdS/FTO/Glass electrode. The results confirm the prospects of enhancing PEC characteristics for the as-deposited flexible CdS electrodes by multi-layer deposition. Such PEC performance improvement is consistent with enhancement in other properties for the flexible CdS film described above.

3.5.2. Annealed electrode

Effect of annealing on PEC characteristics for the flexible four-layered CBD-CdS/ITO/PET electrode has been studied here. High temperatures have been examined for comparison, but the 125 °C shows highest performance and is described here.

Fig. 6 shows photo J-V plots for four-layered CBD-CdS/ITO/PET electrodes, as-deposited, 125 °C annealed and quickly cooled and 125 °C annealed and slowly cooled. The PEC characteristics for each film are summarized Table (2).

Fig. 6 and the Table (entries 1–3) show that annealing the four-layered CdS film at a moderate temperature significantly enhances its J_{SC} value. This behavior resembles earlier results made for other film electrodes, pre-treated only at moderate temperatures, such as those of WSe [49]. The effect is observed in both slow and fast cooling here. The quickly cooled film has higher PEC performance (η 1.20%) than the slowly cooled counterpart (0.83%). The flexible four-layered film also shows superiority to earlier reported rigid CdS films (entries 1–7), which shows the future prospects of using flexible CdS film electrodes once treated properly. Moreover, the Table (entries 1 and 7) shows that the properly treated flexible CdS performance is not far inferior than earlier reported rigid heterojunction solar cells. The PEC behaviors for the three CdS films parallel their physical properties described above. The PEC characteristics, for various semiconducting materials, can be enhanced

Table (2)
Effect of 125 °C annealing and cooling rate on PEC characteristics of flexible four-layered CBD-CdS/ITO/PET electrodes compared with literature.

Entry number	Electrode	Annealing description	V_{OC} (V)	J_{SC} (mA\cm^2)	*FF*	*η*%	*Ref.*
1	CBD-CdS/ITO/PET (four-layered)	As deposited	−0.9	0.095	0.33	0.35	This work
2		125 °C, annealed slowly cooled	−0.7	0.270	0.38	0.83	This work
3		125 °C, annealed quickly cooled	−0.9	0.290	0.40	1.20	This work
4	CBD-CdS/FTO/Glass (mono-layered)	As deposited	−0.33	0.1	0.28		[7]
5		250 °C annealed, slowly cooled	−0.43	0.17	0.27	0.23	[7]
6		150 annealed, slowly cooled	−0.46	0.22	0.30	0.28	[6]
7	Al/PbS/PbS/CdS/ZnO/FTO/glass	Heterojunction	~0.28	~0.028	0.53	4.03	[15]

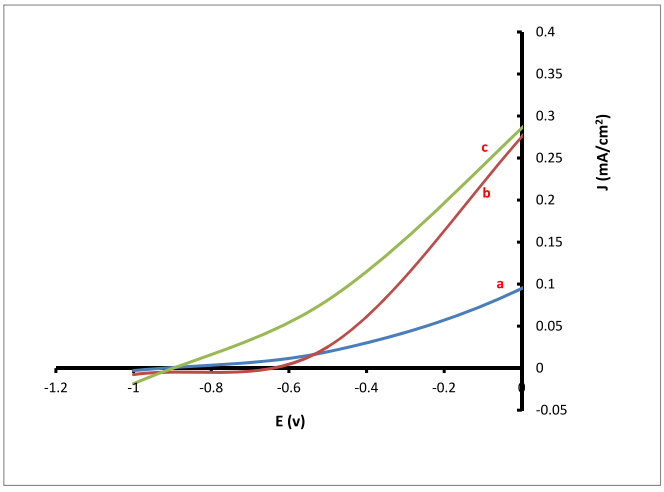

Fig. 6. Photo J-V plots measured for four-layered CBD-CdS/ITO/PET electrodes. (a) as-deposited, (b) 125 °C annealed and slowly cooled, and (c) 125 °C annealed and quickly cooled.

by modifying their physical and chemical properties. For example, TiO_2 characteristics, such as particle sizes and band gaps, can be modified by doping and by varying preparation conditions which consequently affect it photocatalytic efficiency in various applications [50]. CdS semiconductor characteristics, including their band gaps, were modified by doping with Ag, for the purpose of producing thin film electrodes with enhanced PEC characteristics [51]. Moreover, Cr incorporation in copper vanadate was reported to increase its catalytic efficiency in PEC hydrogen production from water splitting [52]. The enhanced PEC characteristics described here therefore result from improved characteristics of the flexible CdS films.

Based on XRD patterns, annealing improves film crystallinity, which rationalizes the improvement in PEC characteristics here. The quickly cooled film exhibits highest PEC performance as it has highest crystallinity among the series. The slowly cooled electrode is superior to the as-deposited film, but has lower crystallinity than the quickly cooled film. With higher film crystallinity, and less imperfections, the quickly cooled CBD-CdS/ITO/PET film should have higher PEC performance. Similar discussions were earlier described for rigid CdS film electrodes [7,23].

Annealing caused densification in the flexible CdS film, which should enhance its conductivity and lower internal resistance. Further internal resistance lowering may also be due to improved adhesion between semiconductor films and the substrate surfaces [53] by annealing. Annealing improves characteristics of other films types [54]. Moreover, annealing increases the agglomerate sizes in the CdS films which improves carrier mobility in the film. To confirm that, resistivity has been measured for the three films, by the four-probe method, and the approximate values are 4.4, 3.8 and 4.1 Ω cm, for the as-deposited, quickly cooled and slowly cooled films, respectively. The measured values resemble those reported for mono-layered CdS films prepared on other substrates and annealed at ~150 °C [55]. With lower resistivity, both annealed films exhibit higher PEC performance values than the as-deposited film, as earlier described for other systems [23]. However, the slowly cooled film exhibits higher resistivity, compared with the quickly cooled film, as described in Table 2 (entries 2 and 3).

All such enhancements in film characteristics, are responsible for improved PEC performance by annealing the four-layered film electrode, despite the lack of crystallite sintering and growth. Similar results were earlier reported for other CdS film electrode properties and PEC characteristics [56].

3.5.3. *Stability of four-layered CdS/ITO/PET electrode*

Based on its special PEC characteristics, the quickly cooled four-layered CBD-CdS/ITO/PET film, its stability under PEC conditions has been studied. Plots of J_{sc} vs. time, measured at (0.0 **V** vs NHE), using the S/Na_2S/NaOH redox couple system, have been used as indicators for electrode stability to corrosion. A stable electrode maintains a steady J_{SC} value for long time, whereas the value lowering indicates less a stable electrode. The measurements, Fig. 7, have been made under low illumination intensity ~0.0086 W cm^{-2} to avoid any possible heating. The Figure shows that the annealed and quickly cooled film exhibits higher J_{SC} value that remains steady with no noticeable decay. In comparison, the as-deposited film exhibits slightly lower J_{SC} values that decay with time. The results confirm the added value of 125 °C annealing, followed by quick cooling, in stabilizing the CdS/ITO/PET electrode.

The film stability enhancement can be rationalized based on improved conversion efficiency for the quickly cooled four-layered film. Under illumination, the semiconductor valence band (VB) electrons are excited to the conduction band (CB) leaving holes behind. The electrons transfer through the film to the PET conducting layer and move through the external connections. On the other hand, the holes are released through the solid/liquid interface to oxidize the Redox couple. With no quick hole release, the holes accumulate in the space charge layer (SCL) and may photo-corrode the electrode. They may also create surface states at the electrode. Such effects lower the short circuit current and consequently the electrode stability. As the quickly cooled electrode exhibits higher J_{SC} value, with lower film resistivity, it exhibits faster hole release between the electrode and the redox couple at the solid/liquid interface. This prevents hole accumulation in the SCL, and

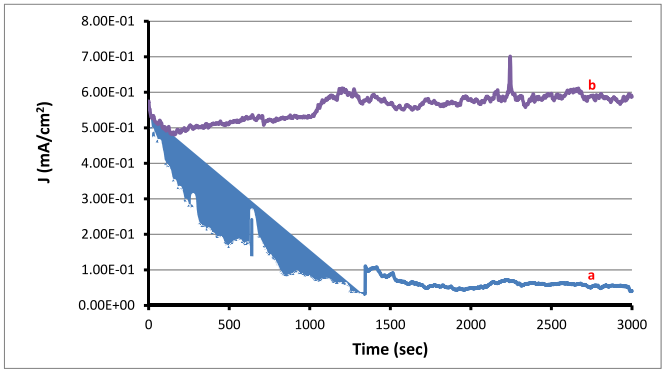

Fig. 7. Stability of CBD-CdS/ITO/PET film electrodes. Profiles show J_{SC} vs time plots for (a) as-deposited and (b) 125 °C annealed and quickly cooled electrodes.

consequently protects the electrode from photo-corrosion. Enhancement in solar cell stability by preventing charge accumulation has been described in other types of solar cells [57,58].

All in all, the results show that the four-layered CBD-CdS/ITO/PET film properties can be enhanced by choosing the proper preparation time, layer number, moderate temperature annealing and quick cooling. PEC characteristics, namely conversion efficiency and stability, can then be significantly improved. The findings indicate the possibility of pristine CdS electrodes, deposited onto flexible substrates to exhibit sound conversion efficiencies and to compete with other rigid CdS systems, and with heterojunction PbS/CdS solar cells. More future work on such CdS electrodes is needed. Effects of layer number, deposition time, annealing and cooling method on film morphology, uniformity and depth profiling, should be further investigated, because film morphology is an important property that affects PEC characteristics [59]. Investigation of other physical properties, such as Hall effect, carrier concentration and others, is underway. Recycling CBD-CdS/ITO/PET electrodes, to preserve the environment and recover both the substrates and the semiconductor material, is also underway here.

4. Conclusion

Pristine CdS films can be prepared onto flexible indium-tin oxide/polyethylenetrephthalte substrates to yield the CdS/ITO/PET films. The chemical bath deposited (CBD) film has more suitable film thickness than the electrochemically deposited (ECD). Effects of preparation time, layer number, annealing and cooling rate on the CBD film characteristics and photoelectrochemical (PEC) performance are described. The four-layered films, each layer prepared in 30 min, shows best characteristics, among various layer preparations. The as-deposited four-layered film electrode shows photoelectrochemical (PEC) activity that is comparable to rigid CdS/FTO/Glass electrodes described earlier, but its stability under PEC conditions is questionable. Fortunately, both the PEC performance and stability of the four-layered CBD-CdS/ITO/PET are significantly improved by moderate temperature annealing and quick cooling to avoid film prolonged exposure to heat. The results show the possibility of the pristine flexible CdS film to compete with other rigid CdS counterparts once treated carefully.

CRediT authorship contribution statement

M. Sbeah: Investigation, Writing original draft.
H.S. Hilal: Supervision, Writing original draft, Correspondence, Project Administration.
A. Zyoud: Supervision, Project Administration.
N. Al Armouzi: Formal analysis.
M. Ishtaiwi: Formal analysis.
M. Haajjyahya: Formal analysis.
H. Nassar: Supervision, Investigation.
N. Qamhieh: Investigation.
A.R. Hajamohideen: Investigation.
S. Zyoud: Validation.
H. Helal: Conceptualization, Formal analysis.
H. Bsharat: Conceptualization, Formal analysis.
M.H.S. Helal: Resources, Data curation, Formal analysis.

Declaration of competing interest

The authors declare that they have no known competing financial interests or personal relationships that could have appeared to influence the work reported in this paper.

Data availability

Data will be made available on request.

Acknowledgement

The results described here are mainly based on M. Sbeah MSc thesis under direct supervision of H. S. Hilal and A. Zyoud, at An-Najah National University. N. Al Armouzi calculated film thickness using the Tauc plot method. M. Ishtaiwi and M. Haajjyahya calculated film thickness from the electronic absorption spectra using the Envelope method. H. Nassar participated in lab training and supervising. N. Qamhieh, A.R. Hajamohideen and S. Zyoud made XRD, SEM and EDS measurement. H. Helal and H. Bsharat participated with conceptualization of the ideas of preparing flexible films and graphics. M.H.S. Helal participated with computer and literature. No special funds have been given to this work.

References

[1] K. Vijayan, S. Vijayachamundeeswari, K. Sivaperuman, N. Ahsan, T. Logu, Y. Okada, A review on advancements, challenges, and prospective of copper and non-copper based thin-film solar cells using facile spray pyrolysis technique, Sol. Energy 234 (2022) 81–102.
[2] K. Rodríguez-Rosales, J. Quiñones-Galván, A. Guillén-Cervantes, E. Campos-González, J. Santos-Cruz, S. Mayén-Hernández, J. Arias-Cerón, M. de la L Olvera, O. Zelaya-Angel, L. Hernández-Hernández, Nanocrystalline-CdS thin films grown on flexible PET-substrates by chemical bath deposition, Mater. Res. Express 4 (2017), 075904.
[3] A. Oliva, O. Solıs-Canto, R. Castro-Rodrıguez, P. Quintana, Formation of the band gap energy on CdS thin films growth by two different techniques, Thin Solid Films 391 (2001) 28–35.
[4] A. Alam, W. Cranton, I. Dharmadasa, Electrodeposition of CdS thin-films from cadmium acetate and ammonium thiosulphate precursors, J. Mater. Sci. Mater. Electron. 30 (2019) 4580–4589.
[5] S. Kumari, D. Suthar, M. Kannan, N. Kumari, M. Dhaka, Understanding the grain growth mechanism in CdS thin films by CdCl2 treatment and thermal annealing evolution, Opt. Mater. 123 (2022), 111900.
[6] A. Zyoud, N.N. Abdul-Rahman, G. Campet, D. Park, H. Kwon, T.W. Kim, H.-J. Choi, M.H. Helal, H.S. Hilal, Enhanced PEC characteristics for CdSe polycrystalline film electrodes prepared by combined electrochemical/chemical bath depositions, J. Electroanal. Chem. 774 (2016) 7–13.
[7] A. Zyoud, I. Saa'deddin, S. Khudruj, Z.M. Hawash, D. Park, G. Campet, H.S. Hilal, CdS/FTO thin film electrodes deposited by chemical bath deposition and by electrochemical deposition: a comparative assessment of photo-electrochemical characteristics, Solid State Sci. 18 (2013) 83–90.
[8] A. Zyoud, I. Saadeddin, S. Khurduj, Z.M. Hawash, M.I. Faroun, G. Campet, D. Park, H.S. Hilal, Combined electrochemical/chemical bath depositions to prepare CdS film electrodes with enhanced PEC characteristics, J. Electroanal. Chem. 707 (2013) 117–121.
[9] K. Znajdek, M. Sibiński, A. Strąkowska, Z. Lisik, Polymer substrates for flexible photovoltaic cells application in personal electronic system, Opto-Electron. Rev. 24 (2016) 20–24.
[10] M. Hassan, G. Abbas, N. Li, A. Afzal, Z. Haider, S. Ahmed, X. Xu, C. Pan, Z. Peng, Significance of flexible substrates for wearable and implantable devices: recent advances and perspectives, Adv. Mater. Technol. 7 (2022), 2100773.
[11] P. Reinhard, A. Chirilă, P. Blösch, F. Pianezzi, S. Nishiwaki, S. Buechelers, A. N. Tiwari, Review of progress toward 20% efficiency flexible CIGS solar cells and manufacturing issues of solar modules, in: 2012 IEEE 38th Photovoltaic Specialists Conference (PVSC) PART 2, IEEE, 2012, pp. 1–9.
[12] F. Ma, Y. Deng, X. Ni, J. Hou, G. Liu, S. Peng, Flexible CdS/CdSe quantum dots sensitized solar cells with high performance and durability, Nano Select 2 (2021) 1347–1355.
[13] H. Li, S. Xiao, J. Zhou, J. Zhao, F. Liu, G. Li, D. Zhang, A flexible CdS nanorods-carbon nanotubes/stainless steel mesh photoanode for boosted photoelectrocatalytic hydrogen evolution, Chem. Commun. 55 (2019) 2741–2744.
[14] K. Acharya, J. Skuza, R. Lukaszew, C. Liyanage, B. Ullrich, CdS thin films formed on flexible plastic substrates by pulsed-laser deposition, J. Phys. Condens. Matter 19 (2007), 196221.
[15] D.H. Yeon, B.C. Mohanty, C.Y. Lee, S.M. Lee, Y.S. Cho, High-efficiency double absorber PbS/CdS heterojunction solar cells by enhanced charge collection using a ZnO nanorod array, ACS Omega 2 (2017) 4894–4899.
[16] M. Ouafi, B. Jaber, L. Laânab, Low temperature CBD growth of CdS on flexible substrates: structural and optical characterization, Superlattice. Microst. 129 (2019) 212–219.
[17] V. Gevorgyan, L. Hakhoyan, N. Mangasaryan, P. Gladyshev, Substrate temperature and annealing effects on the structural and optical properties of nano-CdS films deposited by vacuum flash evaporation technique, Chalcogenide Lett. 13 (2016).
[18] M. Shur, S. Rumyantsev, R. Gaska, B. Wei, R. Vajtai, P. Ajayan, J. Sinius, Structural and transport properties of CdS films deposited on flexible substrates, Solid State Electron. 46 (2002) 1417–1420.
[19] M.S. Hussien, M.I. Mohammed, I.S. Yahia, Flexible photocatalytic membrane based on CdS/PMMA polymeric nanocomposite films: multifunctional materials, Environ. Sci. Pollut. Control Ser. 27 (2020) 45225–45237.
[20] J.-H. Lee, Structural and optical properties of CdS thin films on organic substrates for flexible solar cell applications, J. Electroceram. 17 (2006) 1103–1108.

[21] K. Rodríguez-Rosales, K. Nieto-Zepeda, J. Quiñones-Galván, J. Santos-Cruz, S. Mayén-Hernández, A. Guillen-Cervantes, F. De Moure-Flores, CdS/CdSe HETEROSTRUCTURES GROWN BY CHEMICAL TECHNIQUES ON FLEXIBLE PET/ITO SUBSTRATES, Chalcogenide Lett. 17 (2020) 529–536.
[22] H.S. Hilal, A. Zyoud, M.H. Hilal, H. Bsharat, H. Nassar, A. Cheknane, Charge transfer catalysis at solid/liquid interface in photoelectrochemical processes: enhancement of polycrystalline film electrode stability and performance, Sol. Energy 197 (2020) 443–454.
[23] H.S. Hilal, A. Zyoud, M.H. Helal, H. Bsharat, H.H. Helal, C. Ali, Effects of annealing temperature and cooling rate on photo-electrochemical performance of pristine polycrystalline metal-chalcogenide film electrodes, Sol. Energy 183 (2019) 704–715.
[24] R. Aggarwal, D.K. Kaushik, Structural and optical studies on sol-gel driven spin-coated CdS thin films, in: Journal of Physics: Conference Series, IOP Publishing, 2022, 012012.
[25] A. Ali, A. Mannan, U. Ali Shah, M. Zia, Removal of of toxic metal ions (Ni2+ and Cd2+) from wastewater by using TOPO decorated iron oxide nanoparticles, Appl. Water Sci. 12 (2022) 1–15.
[26] H.S. Hilal, R.M. Ismail, A. El-Hamouz, A. Zyoud, I. Saadeddin, Effect of cooling rate of pre-annealed CdS thin film electrodes prepared by chemical bath deposition: enhancement of photoelectrochemical characteristics, Electrochim. Acta 54 (2009) 3433–3440.
[27] G. Sasikala, R. Dhanasekaran, C. Subramanian, Electrodeposition and optical characterisation of CdS thin films on ITO-coated glass, Thin Solid Films 302 (1997) 71–76.
[28] F. Kadirgan, D. Mao, W. Song, T. Ohno, B. McCANDLESS, Properties of electrodeposited cadmium sulfide films for photovoltaic devices with comparison to CdS films prepared by other methods, Turk. J. Chem. 24 (2000) 21–34.
[29] N. Benderdouche, B. Bestani, B. Benstaali, Z. Derriche, Enhancement of the adsorptive properties of a desert Salsola vermiculata species, Adsorpt. Sci. Technol. 21 (2003) 739–750.
[30] S. Lee, J. Kim, S. Lee, H.-J. Cha, C.-S. Son, Y.-G. Son, D. Hwang, Variations in the physical properties of RF-sputtered CdS thin films observed at substrate temperatures ranging from 25° C to 500° C, Nanomaterials 12 (2022) 1618.
[31] N. Al Armouzi, M. Manoua, H.S. Hilal, A. Liba, M. Mabrouki, Multi-layered sol–gel spin-coated CuO nanofilm characteristic enhancement by Sn doping concentration, Processes 10 (2022) 1277.
[32] S. Ilican, M. Caglar, Y. Caglar, Determination of the thickness and optical constants of transparent indium-doped ZnO thin films by the envelope method, Mater. Sci. Poland 25 (2007) 709–718.
[33] I. Merkulova, Determining thickness and optical properties of a-SiOx thin films by PUMA and envelope method, in: Journal of Physics: Conference Series, IOP Publishing, 2020, 012140.
[34] T. Xu, X. Wei, F. Zhao, G. Wang, Z. Deng, J. Zhao, J. Yao, One-step synthesis of CdS hierarchical microspheres and its ethanol sensing property, Appl. Surf. Sci. 595 (2022), 153545.
[35] F. Ouachtari, A. Rmili, B. Elidrissi, A. Bouaoud, H. Erguig, P. Elies, Influence of bath temperature, deposition time and S/Cd ratio on the structure, surface morphology, chemical composition and optical properties of CdS thin films elaborated by chemical bath deposition, J. Mod. Phys. (2011) 2011.
[36] M. Ouafi, B. Jaber, L. Atourki, N. Zayyoun, A. Ihlal, A. Mzerd, L. Laânab, In situ low-temperature chemical bath deposition of CdS thin films without thickness limitation: structural and optical properties, Int. J. Photoenergy (2018) 2018.
[37] M. Singh, M. Goyal, K. Devlal, Size and shape effects on the band gap of semiconductor compound nanomaterials, J. Taibah Univ. Sci. 12 (2018) 470–475.
[38] H. Jia, Y. Hu, Y. Tang, L. Zhang, Synthesis and photoelectrochemical behavior of nanocrystalline CdS film electrodes, Electrochem. Commun. 8 (2006) 1381–1385.
[39] J.P. Enríquez, X. Mathew, Influence of the thickness on structural, optical and electrical properties of chemical bath deposited CdS thin films, Sol. Energy Mater. Sol. Cell. 76 (2003) 313–322.
[40] A. Zyoud, R.S. Al-Kerm, R.S. Al-Kerm, M. Waseem, H.H. Mohammed, D. Park, G. Campet, N. Sabli, H.S. Hilal, High PEC conversion efficiencies from CuSe film electrodes modified with metalloporphyrin/polyethylene matrices, Electrochim. Acta 174 (2015) 472–479.
[41] M. Thirumoorthi, J. Thomas Joseph Prakash, Structure, optical and electrical properties of indium tin oxide ultra thin films prepared by jet nebulizer spray pyrolysis technique, J. Asian Ceram. Soc. 4 (2016) 124–132.
[42] Z. Ghorannevis, E. Akbarnejad, M. Ghoranneviss, Structural and morphological properties of ITO thin films grown by magnetron sputtering, J. Theoret. Appl. Phys. 9 (2015) 285–290.
[43] A. Antony, Preparation and Characterisation of Certain II-VI, I-III-VI2 Semiconductor Thin Films and Transparent Conducting Oxides, Department of Physics Cochin University of Science and Technology Cochin–682022, Kerala, India, 2004.
[44] I. Oladeji, L. Chow, J. Liu, W. Chu, A. Bustamante, C. Fredricksen, A. Schulte, Comparative study of CdS thin films deposited by single, continuous, and multiple dip chemical processes, Thin Solid Films 359 (2000) 154–159.
[45] T. Semikina, Fabrication of CdS/CdTe solar cells by quasiclosed space technology and research of their properties, Ukrainian J. Phys. (2018) 156–167.
[46] A.S. Gadalla, H.A. Al-shamiri, S.M. Alshahrani, H.F. Khalil, M.M. El Nahas, M. A. Khedr, Epitaxial growth and optical properties of laser deposited CdS thin films, Coatings 12 (2022) 87.
[47] K.S. Ramaiah, R. Pilkington, A. Hill, R. Tomlinson, A.-K. Bhatnagar, Structural and optical investigations on CdS thin films grown by chemical bath technique, Mater. Chem. Phys. 68 (2001) 22–30.
[48] S. Rajpal, V. Bandyopadhyay, Structural and Optical Properties of CdS Thin Film Grown by Chemical Bath Deposition, Журнал нано-та електронної фізики, 2013, 03021-03021-03021-03023.
[49] M.A. Khan, M.Q. Mehmood, Y. Massoud, High-temperature annealing effects on atomically thin tungsten diselenide field-effect transistor, Appl. Sci. 12 (2022) 8119.
[50] M. Ijaz, M. Zafar, Titanium dioxide nanostructures as efficient photocatalyst: progress, challenges and perspective, Int. J. Energy Res. 45 (2021) 3569–3589.
[51] T. Iqbal, G. Ara, N. Khalid, M. Ijaz, Simple synthesis of Ag-doped CdS nanostructure material with excellent properties, Appl. Nanosci. 10 (2020) 23–28.
[52] T. Iqbal, A. Hassan, M. Ijaz, M. Salim, M. Farooq, M. Zafar, M. Tahir, Chromium incorporated copper vanadate nano-materials for hydrogen evolution by water splitting, Appl. Nanosci. 11 (2021) 1661–1671.
[53] A.M. Ali, M. Egiza, K. Murasawa, H. Sugita, T. Deckert-Gaudig, V. Deckert, T. Yoshitake, Effects of substrate temperature and intermediate layer on adhesion, structural and mechanical properties of coaxial arc plasma deposition grown nanodiamond composite films on Si substrates, Surf. Coating. Technol. 417 (2021), 127185.
[54] R. Wang, Z. Xia, X. Kong, L. Liang, K.K. Ostrikov, Etching and annealing treatment to improve the plasma-deposited SiOx film adhesion force, Surf. Coating. Technol. 427 (2021), 127840.
[55] V. Canevari, N. Romeo, G. Sberveglieri, S. Azzi, A. Tosi, M. Curti, L. Zanotti, Low resistivity CdS thin films grown by flash-evaporation at low substrate temperature (150–200° C), J. Vac. Sci. Technol.: Vac. Surf. Films 2 (1984) 9–10.
[56] A. Zyoud, S. Al-Yamani, H. Bsharat, M.H. Helal, H. Kwon, D. Park, H.S. Hilal, Recycled polycrystalline CdS film electrodes with enhanced photo-electrochemical characteristics, Mater. Sci. Semicond. Process. 74 (2018) 277–283.
[57] D. Xue, M. Saito, I. Osaka, K. Marumoto, Stability improvement mechanism due to less charge accumulation in ternary polymer solar cells, npj Flexib. Electr. 6 (2022) 1–10.
[58] S. He, S. Li, A. Zhang, G. Xie, X. Wang, J. Fang, Y. Qi, L. Qiu, Residual strain reduction leads to efficiency and operational stability improvements in flexible perovskite solar cells, Mater. Adv. 3 (2022) 6316–6323.
[59] Y. Tang, Z. Gu, C. Fu, Q. Xiao, S. Zhang, Y. Zhang, Y. Song, FAPbI3 perovskite solar cells: from film morphology regulation to device optimization, Solar RRL 6 (2022), 2200120.